

Mapping of Surface Potentials by Electrons on a Helium Film

E. Teske, P. Leiderer¹, P. Wyder and V. Shikin²

Grenoble High Magnetic Field Laboratory, Max-Planck-Institut für Festkörperforschung/Centre National de la Recherche Scientifique, B.P.166, F-38042 Grenoble Cedex 9, France.

¹*Fakultät für Physik, Universität Konstanz, D-78434 Konstanz, Germany.*

²*Institute of Solid State Physics, 142432 Chernogolovka, Moscow District, Russia.*

A novel way to investigate perturbations of the electrostatic potential across a sample surface is presented, aiming at application in 2D contact phenomena. The idea is to deposit surface state electrons (SSE) on a thin layer of liquid helium covering the surface of a solid state sample. The density of the SSE adjusts to screen perturbations of the electrostatic potential across the sample. As a result, the helium layer thickness varies due to the variation of the electrostatic pressure, thus providing a map. This map may be read interferometrically by a technique already employed for the investigation of multi-electron dimples on helium. We realized this mapping for a structured metal electrode as a test sample to investigate the resolution of the method.

PACS numbers: 68.10.Gw, 73.90.+f, 67.90.+z

1. INTRODUCTION

Contact phenomena, a quite well-known feature in 3D metal and semiconductor physics, may have special significance for the behaviour of 2D conducting systems. In 3D systems the accompanying perturbation of charge carrier density is strongly localised within a very small distance (Debye radius) from the interface. In 2D systems instead, this perturbation has a macroscopic range, extending easily over a large fraction of the whole system. This phenomenon may be of great importance for transport measurements in low dimensional electron systems, as for example the Quantum Hall Effect, different size effects, etc.

A means to investigate this effect is the mapping of the electrostatic

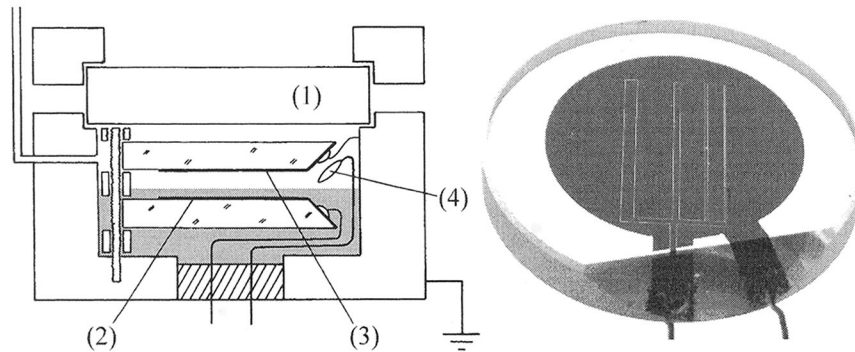


Fig. 1. Left: Drawing of the sample cell. Right: Picture of electrode with interdigital structure. The diameter of the evaporated metal area is 2 cm. The widths of the stripes are 1 mm, 0.5 mm, 0.2 mm and 0.1 mm. The meaning of the numbers is explained in the text.

potential across the sample surface. Here one could think of employing the screening properties of electrons on a layer of liquid helium. In favour of this method would be the possibility to realise it under DC conditions and without complete screening of the substrate potential, unlike alternative techniques, based, for example, on the linear electro-optic effect¹⁻³.

In the following we will describe this method based on experimental data and calculations for a structured metal electrode as a test sample.

2. EXPERIMENT

Fig. 1 shows the details of the experimental setup. To measure the helium surface topology we employed an interferometrical technique similar to the one used in other experiments⁴. Inside the cell, two glass plates with evaporated metal electrodes (2,3) are mounted to form a horizontally aligned plane capacitor with a spacing of 4 mm partly filled by a layer of liquid helium. The bottom electrode (2), consisting of a 150 nm thick gold layer, serves as a highly reflective mirror while the top electrode (3), a 20 nm thick silver layer, acts as a partly reflective mirror with a transmission/reflection ratio of about 25%. Through a window (1), the interior of the sample cell is illuminated by coherent light ($\lambda = 632.8$ nm), giving rise to interference between light directly reflected off the top electrode and light reflected off the bottom electrode. The phase shift between these beams has a component γ depending on the local thickness d of the helium layer above

the bottom plate, given by $\gamma = \frac{2\pi}{\lambda} (n_l - n_g) 2d = 2\pi \frac{d}{15 \mu\text{m}}$, where $n_l = 1.0243$ and $n_g = 1.0032$ are the refractive indices of liquid and gaseous helium at the experimental temperature of 4.2 Kelvin.

Deformations of the helium surface are thus visible in shifts of the interference pattern, where the distance between two fringes corresponds to a deformation of 15 μm . This value gives a first estimate of the height resolution of this method. To further improve the resolution, the transmission/reflection ratio of the top electrode has been chosen comparatively low, which results in multiple beam interference, as in a Fabry-Perot interferometer, and strongly narrows the black fringes in the interference pattern. Thus, an improvement in resolution by about one order of magnitude was achieved, enabling the detection of surface deformations down to below 1 μm .

To charge the helium surface, a DC holding potential V is applied between top and bottom metal electrode, and a field emission tip (4) is used to inject free electrons into the vapor space above the helium surface. The electrons are drawn onto the helium surface where they form a charge layer of initially homogeneous areal density, producing an equally homogeneous electrostatic pressure on the helium surface.

To examine the influence of an additional potential variation across the lower electrode, and to model the conditions for the investigation of 2D contact phenomena, this electrode was lithographically structured with an interdigital pattern, displayed on the right in Fig. 1, where a small additional potential ΔV relative to the rest of the electrode can be applied. The resulting disturbance of the initially homogeneous electrostatic field and charge density across the helium surface then leads to redistribution of the local electrostatic pressure and becomes visible in a corresponding surface deformation, as shown in Fig. 2.

3. THEORY

In the following we will calculate the shape of the charged helium surface across one stripe of the interdigital structure shown in Fig. 1.

Let x be the spatial coordinate perpendicular to the stripe axis, with the stripe itself between $x = -w$ and $x = +w$, and let the helium surface be at an equilibrium height d above the bottom electrode. The local height $\eta(x)$ of the charged helium surface across the stripe is determined by the equilibrium between surface tension, gravitation and electrostatic force,

$$\frac{d^2}{dx^2}\eta(x) - \kappa^2\eta(x) = \frac{1}{8\pi\alpha} (E_-(x))^2, \quad \kappa = \sqrt{\frac{\rho g}{\alpha}}, \quad (1)$$

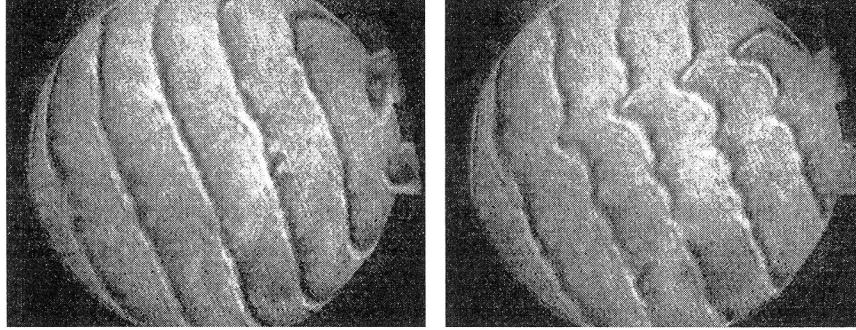


Fig. 2. Interferometric images with electrode from Fig. 1. The stripes of the structure (not visible here) are aligned perpendicular to the fringes. Left: $\Delta V = 0$ Volts; Right: $\Delta V = 0.4$ Volts. He layer thickness $d = 45 \mu\text{m}$.

where α is the coefficient of surface tension, ρ is the density of liquid helium, g is the acceleration of gravity and κ is the capillary constant. $E_-(x)$ is the electrostatic field immediately below the helium surface.

To determine $E_-(x)$ one has to take into account the overall holding potential V on the bottom electrode, the potential perturbation $V_1(x)$ introduced by applying additionally ΔV on the stripe, and the layer thickness variation $\eta(x)$ itself. For small perturbations $\Delta V \ll V$ these three contributions can be regarded as mutually independent and $E_-(x)$ can be expressed as the sum $E_-(x) = E_0 + E_1(x) + E_2(x)$, where $E_0 = \frac{V}{d}$ is the equilibrium holding field, $E_1(x)$ describes only the effect of the potential perturbation $V_1(x)$ while neglecting layer thickness changes, and $E_2(x)$ describes solely the effect of the layer thickness variation $\eta(x)$.

In Fourier representation, E_1 can be expressed for an arbitrary shape of the perturbation potential V_1 along the bottom electrode by⁵

$$E_1(q) = \frac{q}{\sinh(qd)} V_1(q) \quad (2)$$

where $V_1(q)$ is the Fourier transform of the perturbation potential.

Similarly, the contribution E_2 due to charge redistribution as the layer thickness η changes can be expressed in Fourier representation as

$$E_2(q) = -E_0 q \coth(qd) \eta(q) \quad (3)$$

Inserting (2) and (3) into the Fourier transform of (1), one arrives at a general expression for $\eta(q)$ in terms of $V_1(q)$ and q . However, for our purposes it

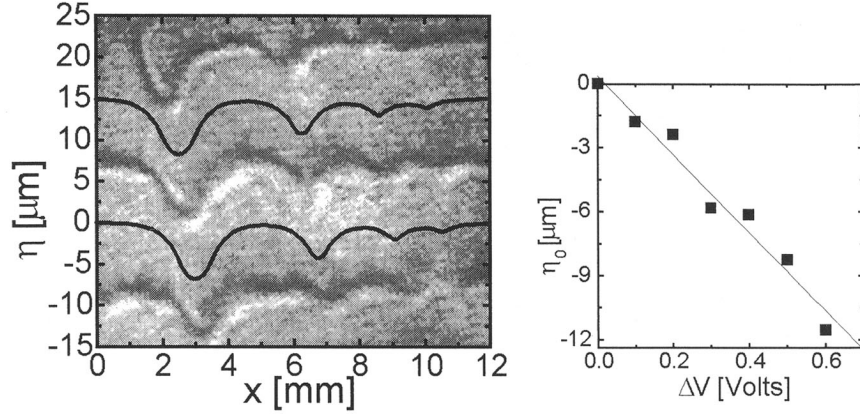


Fig. 3. Left: Calculation compared to original image. Right: Measurement of deformation depth against applied perturbation voltage ($d = 100 \mu\text{m}$).

suffices to consider only the case $\kappa d \ll 1$ which leads to

$$\eta(q) = - \left(\frac{1}{4\pi\alpha} \frac{E_0}{d} \right) \frac{V_1(q)}{q^2 + \kappa_*^2} \quad (4)$$

with a renormalised capillary constant $\kappa_* = \kappa \sqrt{1 - E_0^2/E_c^2}$, where $E_c = \sqrt{4\pi\rho g d}$ is the so-called critical field of the electrohydrodynamic instability⁶.

For the box-shaped potential $V_1(x)$ across the stripe, (4) reduces to

$$\eta(x) = \Delta V \left(\frac{1}{4\pi\alpha\kappa_*^2} \frac{E_0}{d} \right) \cdot \begin{cases} e^{-\kappa_* w} \cosh(\kappa_* x) - 1 & , \text{if } |x| \leq w \\ -e^{-\kappa_* |x|} \sinh(\kappa_* w) & , \text{if } |x| \geq w \end{cases} \quad (5)$$

4. DISCUSSION

To compare Eq. (5) with the experimental results, Fig. 3 shows on the left a calculation of the surface shape across the whole of the structure from Fig. 1, plotted in the original image from Fig. 2. In the calculation, all parameters are fixed except for the value of the holding field E_0 , which cannot be measured directly in our setup. Assuming a relation $E_0^2 = 0.6 \cdot E_c^2$ for maximum possible charging, as seems reasonable also from other reports⁷, there is good agreement between calculation and original image, regarding the shape for the individual stripe with its decay length of κ^{-1} as well as the decrease of overall deformation depth for stripes narrower than κ^{-1} .

The right of Fig. 3 shows a measurement of maximum deformation depth η_0 as a function of the applied perturbation voltage ΔV for another, very broad stripe structure (not depicted), confirming the linear dependence predicted by (5) within experimental error. A fit to the data (drawn line) gives a value of $18.3 \mu\text{m}/\text{Volt}$, in agreement with (5) for $E_0^2 = 0.61 \cdot E_c^2$.

5. CONCLUSIONS

So far, the setup described for potential mapping has a spatial resolution in the range of several tens of millivolts. It should be possible to improve this value by at least one order of magnitude through fine-tuning of the optical setup, a more sophisticated image analysis and improved vibration isolation to reduce oscillations of the helium surface. However, the influence of surface tension tends to smooth out the original shape of the potential perturbation and makes it increasingly difficult to resolve perturbations extending over distances smaller than the capillary length $\kappa^{-1} \approx 0.5 \text{ mm}$.

ACKNOWLEDGMENTS

One of the Authors (V. Shikin) thanks the MPI Grenoble for invitation and financial support. This activity is partly supported by INTAS 93-939 and by NASA-PSA NAS 15-10110, project TM-17.

REFERENCES

1. P. F. Fontein, P. Hendriks, F. A. P. Blom, I. K. Wolter, L. I. Giling, C. W. I. Beenaker, *Surf. Sci.* **963**, 91 (1992).
2. R. Knott, W. Dietsche, K. v. Klitzing, K. Plong, K. Eberle, *Semic. Sci. Technol.* **10**, 117 (1995).
3. W. Dietsche, K. v. Klitzing, U. Ploog, *Surf. Sci.* **361/362**, 289 (1996).
4. P. Leiderer, W. Ebner, V. Shikin, *Surf. Sci.* **113**, 405 (1982).
5. P. M. Morse, H. Feshbach, *Methods of Theoretical Physics*, New York, *McGraw-Hill* (1953).
6. D. M. Chernikowa, *Sov. JLTP* **2**, 669 (1976).
7. A. P. Volodin, M. S. Khaikin, V. S. Edelman *JETP Lett.* **26**, 543 (1977).